Journal of Applied Polymer Science

Synthesis, characterization and, swelling behavior of semi-IPN nanocomposite hydrogels of alginate with poly(*N*-isopropylacrylamide) crosslinked by nanoclay

Meltem Kasapoglu Calik, Murat Ozdemir
Department of Chemical Engineering, Gebze Technical University, Gebze, Kocaeli, 41400, Turkey
Correspondence to: M. Ozdemir (E-mail: ozdemirm@gtu.edu.tr)

ABSTRACT: pH and temperature responsive nanocomposite hydrogels were synthesized with sodium alginate (NaAlg), *N*-isopropylacrylamide (NIPA), and nanoclay. The structure, morphology, thermal behavior, and swelling and deswelling behaviors of the hydrogels were studied. The NaAlg*m*/PNIPA/Clay*n* hydrogels revealed a highly porous structure in which the pore sizes decreased and the amount of pores increased with increasing the nanoclay content in the hydrogels. PNIPA retained its own characteristics regardless of the amount of NaAlg and nanoclay. The effect of pH and nanoclay content on the swelling and effect of temperature on the deswelling behavior were investigated. The equilibrium swelling ratios of the nanocomposite hydrogels increased with increasing the pH from 2 to 6. The maximum swelling was attained at pH 6. Deswelling increased with increasing the nanoclay content in the hydrogels. The hydrogels were found to be pH and temperature responsive. © 2015 Wiley Periodicals, Inc. J. Appl. Polym. Sci. **2016**, *133*, 43222.

KEYWORDS: hydrophilic polymers; properties and characterization; stimuli-sensitive polymers; swelling

Received 11 August 2015; accepted 11 November 2015
DOI: 10.1002/app.43222

INTRODUCTION

Polymer hydrogels are cross-linked hydrophilic networks that can swell, absorb, and retain large amount of aqueous fluids without dissolving.[1] Responsive hydrogels have the capability to change their swelling behavior and other properties in response to external stimuli such as temperature, pH, solvent composition, electromagnetic radiation, and pressure. Because of their useful properties, hydrogels have received great attention in technology,[2] bioengineering,[3] biotechnology,[4] pharmacy,[5] agriculture,[6] food industry,[7] and other fields. Among all the responsive hydrogels, pH and temperature responsive hydrogels have been extensively studied because both pH and temperature are important environmental factors, and they can be easily controlled and applicable both *in vivo* and *in vitro* studies.[8,9]

Poly(*N*-isopropylacrylamide) (PNIPA) is a non-toxic thermosensitive polymer whose swelling behavior changes with respect to temperature.[10,11] It exhibits a phase transition at its lower critical solution temperature (LCST), approximately 32°C.[12] PNIPA readily swells in an aqueous medium and expands in size when the solution temperature is below its LCST, but it shrinks and turns in a compact structure by dehydration when the solution temperature is above its LCST. Due to its temperature responsive property, PNIPA hydrogels have been used in many fields such as pharmaceutical, cosmetics, and food industries.

Sodium alginate (NaAlg) is a naturally derived linear, non-toxic, renewable, water soluble, biodegradable, and biocompatible polysaccharide. It can be extracted from marine algae or produced by bacteria. Alginates form mechanically stable hydrogel networks in presence of divalent cations, such as Ca^{2+}, Mg^{2+}, and Ba^{2+}. Divalent cations act as crosslinkers between the functional groups of alginate chains. Alginates comprised of two different kinds of monomers having carboxylic groups, L-mannuronic and L-guluronic acids. These monomers can form several possible arrangements of chain segments which generate alginates with different gelation properties. Unlike the other natural polysaccharides, alginate has a high gel porosity that allows for high diffusion rates of macromolecules. Its dissolution and biodegradation properties enable it to be used as a matrix for the entrapment and delivery of proteins, drugs and cells.[13] NaAlg can be easily modified through various chemical or physical methods such as direct cross-linking, grafting copolymerization with hydrophilic vinyl monomers, polymer blending and compounding with other functional components.[14] Due to these unique properties, alginates are preferred over the other polysaccharides in synthesis of semi-IPN hydrogels.

The interpenetrating polymer network (IPN) technology is a combination of two polymers where at least one of the polymers is cross-linked in the presence of another.[15] In semi-IPN

systems, there is no chemical bond between components and each polymer network can be sensitive independently to the different external stimuli, such as pH and temperature.[16] The interpenetration of two networks may lead to higher mechanical strength,[17] and improved pH and temperature responsive swelling/deswelling[18] behavior compared with conventional PNIPA hydrogels. The semi-IPN hydrogels with non-toxic synthetic polymers can be a promising alternative in a wide range of applications because of their high sensitivity to external stimuli, good biocompatibility and biodegradability. In recent years, particular interest has been focused to the semi-IPN hydrogels. In these semi-IPN hydrogels, one component is a natural polysaccharide such as chitosan,[19] carboxymethyl chitosan,[20] and sodium alginate,[21] but PNIPA were always cross-linked by an organic cross-linker. These conventional PNIPA hydrogels prepared using organic cross-linkers have several limitations such as weak and brittle mechanical properties, and slow response rates. On the other hand, polymer-clay nanocomposite hydrogels exhibit remarkably improved mechanical and thermal properties, and improved release rates when compared with conventional hydrogels.

Nano-size clays in hydrogels easily disperse in hydrogel structures compared with conventional microsize clays that form aggregates and agglomerates because of the heterogeneous dispersion of clay particles.[22,23] Mechanical properties, thermal stability, and swelling and deswelling behavior of hydrogels can be improved by using nanoclays.[24,25] Another advantage of using nanoclay is that it acts as an inorganic cross-linker, and overcomes the use of organic cross-linkers such as *N,N′*-methylene-*bis*-acrylamide which is toxic when inhaled, swallowed, or ingested and classified as a hazardous material according to Directives 67/548/EEC and 1999/45/EC. To overcome the toxic effects and health risks of *N,N′*-methylene-*bis*-acrylamide, a nanocomposite hydrogel consisting of PNIPA and Laponite was developed where the hydrogel was prepared by *in situ* free radical redox polymerization without using any organic cross-linker.[26] The clay sheets acted as multifunctional cross-linkers for the polymer. The nanocomposite hydrogels exhibited extraordinary mechanical properties with high mechanical strength, high degrees of swelling and also rapid shrinking capacity.[26–29] These nanocomposite hydrogels could be used as smart delivery devices in several applications including drug delivery and delivery of active agents (antimicrobials, antioxidants, nutraceuticals, etc.) in intelligent food packaging.

Bentonite nanoclay is a highly pure aluminosilicate mineral which has a sheet type structure with high aspect ratio, large specific surface area and high cation exchange capacity. The nanoclay consists of about 1 nm thick layers surface substituted with metal cations and stacked in about 10 nm sized multilayer stacks. The stacks can be dispersed in a polymer matrix to form polymer–clay nanocomposite. Bentonite nanoclay because of its low cost and unique properties is a preferred inorganic cross-linker over the other nanoclays such as Laponite. The high price of Laponite limits its use as an inorganic cross-linker in industrial applications.

Recently, the swelling behavior of superabsorbent nanocomposites with five different clays including vermiculite, montmorillonite (bentonite), mica, kaolin, and attapulgite was investigated. Results showed that the type of clay affected the swelling rate differently and montmorillonite composites displayed the highest swelling rate.[30] When compared with others its low cost and superior characteristics such as high water adsorption, extensive swelling in water and higher cation exchange capacity, bentonite as inorganic layered nanoclay has unique advantages over the other clays.

In this work, to combine the advantages of synthetic and natural polymers, a novel pH and temperature responsive semi-IPN hydrogels were synthesized using NaAlg and *N*-isopropylacrylamide (NIPA) as monomers and bentonite nanoclay as a multifunctional inorganic cross-linker instead of conventional organic cross-linkers. Poly(N-isopropylacrylamide) and NaAlg were used as the temperature responsive and pH responsive components of nanocomposite hydrogel system, respectively, to obtain pH- and temperature responsive polymers. The objectives of this work were to: (1) investigate the structure, morphology and thermal behavior of these nanoclay cross-linked hydrogels and (2) study the effect of pH and nanoclay content on the swelling and effect of temperature on the deswelling behavior of these novel hydrogels.

EXPERIMENTAL

Materials

N-isopropylacrylamide (NIPA) was purchased from ABCR (Karlsruhe, Germany). NaAlg was kindly provided by GMT food (Istanbul, Turkey). Potassium peroxodisulfate (KPS) and tris(hydroxymethyl)aminomethane (TRIS) were purchased from Merck (Darmstadt, Germany). Sodium acetate trihydrate ($CH_3COONa{\cdot}3H_2O$) was supplied from JT Baker (Phillipsburg, NJ, USA). *N,N,N′,N′*-tetramethylethylene diamine (TEMED), acetic acid, calcium chloride ($CaCl_2$), hydrochloric acid (HCl), and Nanomer® PGV (bentonite nanoclay, > 98% montmorillonite) were purchased from Sigma-Aldrich (St. Louis, MO, USA). The Nanomer® PGV is a product of Nanocor Inc. (Arlington Heights, IL). It has a thickness of 1 nm, specific gravity = 2.6, cation exchange capacity = 145 meq/100 g and individual sheets have aspect ratios (*L/W*) varying from 150 to 200. All reagents were analytical grade and used as received. All solutions used in the experiments were prepared with deionized water.

Buffer solutions with pH = 2 and pH = 10 were purchased from JT Baker (Phillipsburg, NJ). Buffer solutions with pH = 4 and pH = 6 were consisted of acetic acid ($C = 0.1M$) and the buffer solution with pH = 8 was composed of TRIS ($C = 0.1M$). HCl ($0.1M$) and $CH_3COONa{\cdot}3H_2O$ ($0.1M$) were used to adjust pH. The pH values of the buffer solutions were checked with a pH meter (Mettler-Toledo, SevenEasy model S20, Schwerzenbach, Switzerland).

Preparation of Nanocomposite Hydrogels

Nanocomposite hydrogels were synthesized in polypropylene (PP) test tubes (interior diameter of 10 mm and length of 30 mm) by free radical solution polymerization of NIPA monomer by using KPS as the initiator, nanoclay as the cross-linking agent and TEMED as the accelerator. In the preparation of the nanocomposite hydrogels, the initial dispersion consisting of

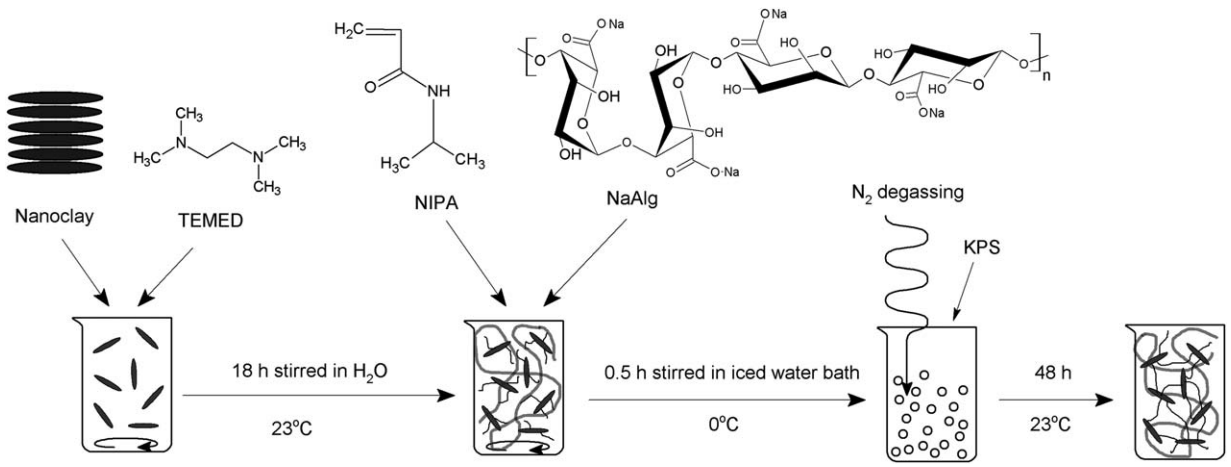

Scheme 1. Synthesis of nanocomposite hydrogels.

TEMED (4 μL), deionized water (0.7 mL) and nanoclay (10, 15, 20 and 30% by weight with respect to NIPA) were stirred with a vortex mixer at 23°C for 18 hours. Then, NIPA monomer (0.1 g), NaAlg (10% and 20% by weight with respect to NIPA) and deionized water (0.3 mL) were added to the dispersion. The dispersion was stirred in an iced-water bath for 30 min until a homogeneous dispersion was obtained. The dispersion was degassed with nitrogen for 15 min to remove dissolved oxygen. Finally, 50 μL KPS (0.06 g in 1 mL H_2O) was added to the dispersion to initiate polymerization. The free radical polymerization was carried out in a water bath at 23°C for 48 hours. At this stage, the complete polymerization/cross-linking of NIPA took place with nanoclay and NaAlg chains remain entrapped within the PNIPA network. Scheme 1 shows the synthesis of nanocomposite hydrogels.

The hydrogels cross-linked by nanoclay are expressed as NaAlg*m*/PNIPA/Clay*n* hydrogels. The letters *m* and *n* correspond to the weight percent of NaAlg and nanoclay with respect to NIPA monomer, respectively. The compositions of prepared nanocomposite hydrogels are given in Table I.

After polymerization was completed, the top plaque above the polymerized hydrogels was removed, and the hydrogels were immersed in an aqueous $CaCl_2$ solution (0.03 g/mL) for 15 min to allow interpenetration of PNIPA network in the alginate-Ca^{2+} network where Ca^{2+} act as a cross-linker between the functional groups of alginate chains. The nanocomposite hydrogels were then immersed in an excess of deionized water for 4 days to remove linear polymer chains and residual unreacted constituents by changing the water daily. Finally, the equilibrium swollen hydrogels were dried in a desiccator at room temperature for a week while the hydrogels for SEM and XRD analysis were dried in a freeze-dryer. The dried hydrogels were kept in a desiccator under vacuum until they were used.

Scanning Electron Microscope (SEM) Analysis

The equilibrium swollen hydrogels in deionized water were freeze-dried under vacuum using a freeze dryer (Virtis Ultra Super XL, New York) at −35°C for overnight. The dried samples were fractured and coated with a thin layer of gold prior to analysis. The structure and morphology of the hydrogels were analyzed by a scanning electron microscope (SEM) (Philips XL30 FEG, Oregon, USA) operating at a voltage of 2 kV.

Thermal Analysis (Measurement of LCST and Glass Transition Temperature, T_g)

The hydrogels were reimmersed in deionized water at room temperature and allowed to swell for at least 24 hours. The LCST and T_g of the hydrogels were measured using a differential scanning calorimeter (DSC) (Perkin Elmer Jade DSC, Shelton,

Table I. Composition of Nanocomposite Hydrogels

		Composition		
Formulation code	Polymer system	NaAlg (g)	NIPA (g)	Nanoclay (g)
A	NaAlg10/PNIPA/Clay10	0.01	0.1	0.01
B	NaAlg20/PNIPA/Clay10	0.02	0.1	0.01
C	NaAlg10/PNIPA/Clay15	0.01	0.1	0.015
D	NaAlg20/PNIPA/Clay15	0.02	0.1	0.015
E	NaAlg10/PNIPA/Clay20	0.01	0.1	0.02
F	NaAlg20/PNIPA/Clay20	0.02	0.1	0.02
G	NaAlg10/PNIPA/Clay30	0.01	0.1	0.03
H	NaAlg20/PNIPA/Clay30	0.02	0.1	0.03

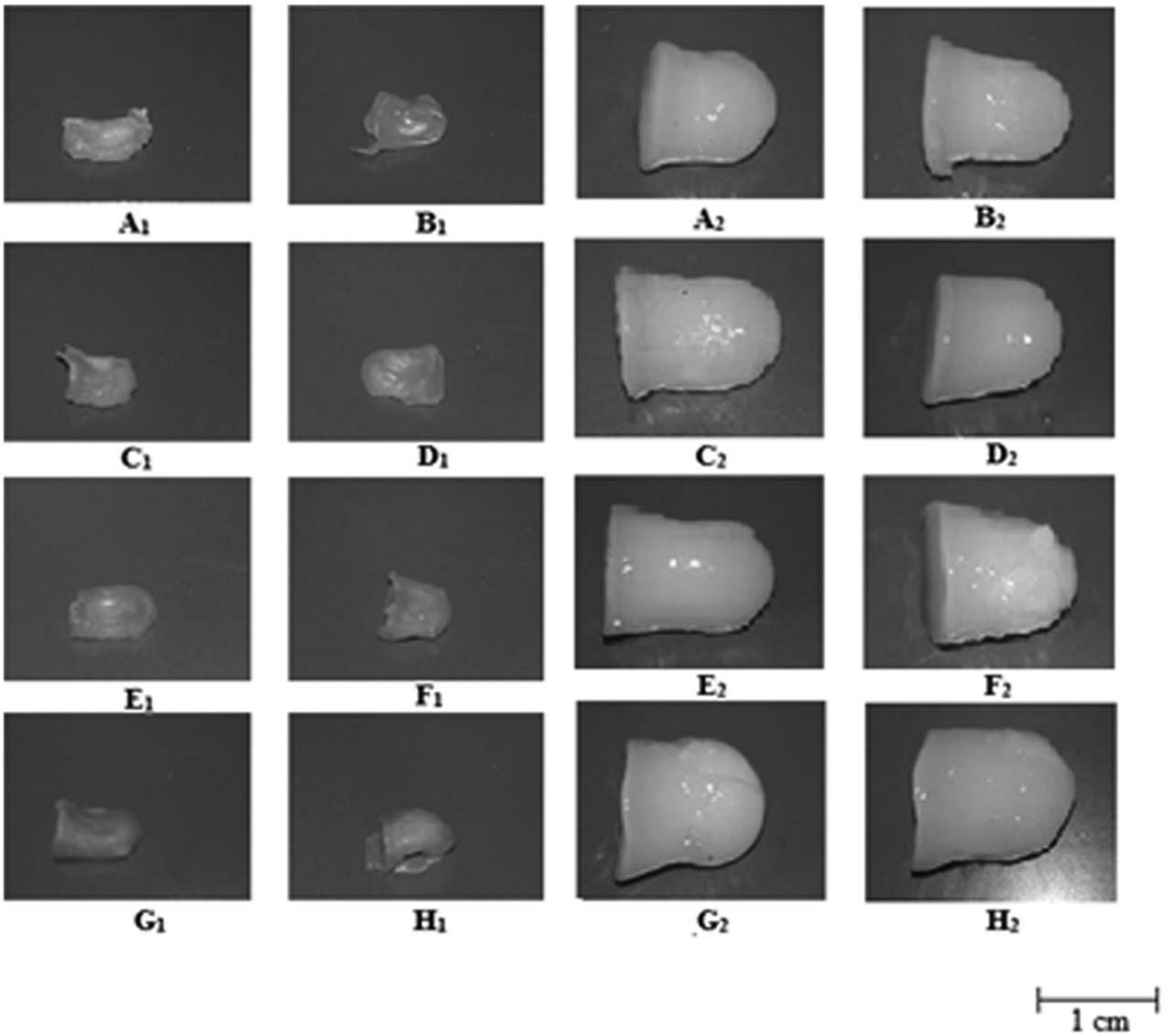

Figure 1. Dried (A_1–H_1) and swollen (A_2–H_2) hydrogels. Subscript 1 shows dried and subscript 2 shows swollen hydrogels based on the codes given in Table I.

CT, USA). The LCST values of the swollen hydrogels were performed from 20 to 45°C at a heating rate of 3°C/min under nitrogen with a flow rate of 25 mL/min to avoid oxidation. Deionized water was used as the reference in DSC analysis.

For the determination of T_g values of the dried hydrogels, approximately 10 mg of dried sample was scanned at a heating rate of 15°C/min under nitrogen with a flow rate of 25 mL/min to prevent oxidation. The first scan was done from 50 to 150°C to remove all residual moisture and erase any thermal history. The T_g values were determined from the second scan performed from 30 to 300°C.

Fourier Transform near Infrared (FT-NIR) Analysis

The dried hydrogels were directly analyzed using a Fourier transform near infrared (FT-NIR) spectrometer (Bruker Optics, Ettlingen, Germany) in the range of 12,500–4000 cm^{-1}.

X-ray Diffraction Analysis

The dried hydrogel samples were milled prior to X-ray diffraction (XRD) analysis. XRD patterns of dried and milled hydrogel samples were determined with an X-ray diffractometer (Rigaku D-max 2200PC, Tokyo, Japan) equipped with an X-ray source of Cu K_α radiation with a wavelength, $\lambda = 1.5418$ Å. Data were collected from 2θ of 5 to 25° (θ being the angle of diffraction) with a scanning rate of 1.2°/min. The voltage and current of the X-ray tubes were 40 kV and 40 mA, respectively.

Determination of Swelling and Deswelling

The dried hydrogels (about 0.06 g) were weighed and immersed in 50 ml of buffer solutions with pH values of 2, 4, 6, 8 and 10. They were placed in a climate controlled cabinet (Sanyo, model MLR-351H, Japan) at 5 ± 0.5°C for 150 h. The hydrogels were removed from the buffer solutions periodically, blotted with a filter paper to remove excess water and weighed. The swelling capacities of hydrogels are expressed in terms of swelling ratio (SR) calculated as grams of water per gram of dried hydrogel as follows:

$$SR = \frac{W_t - W_d}{W_d}$$

where W_t is the weight of the hydrogel at a given time during swelling and W_d is the weight of the dry hydrogel.

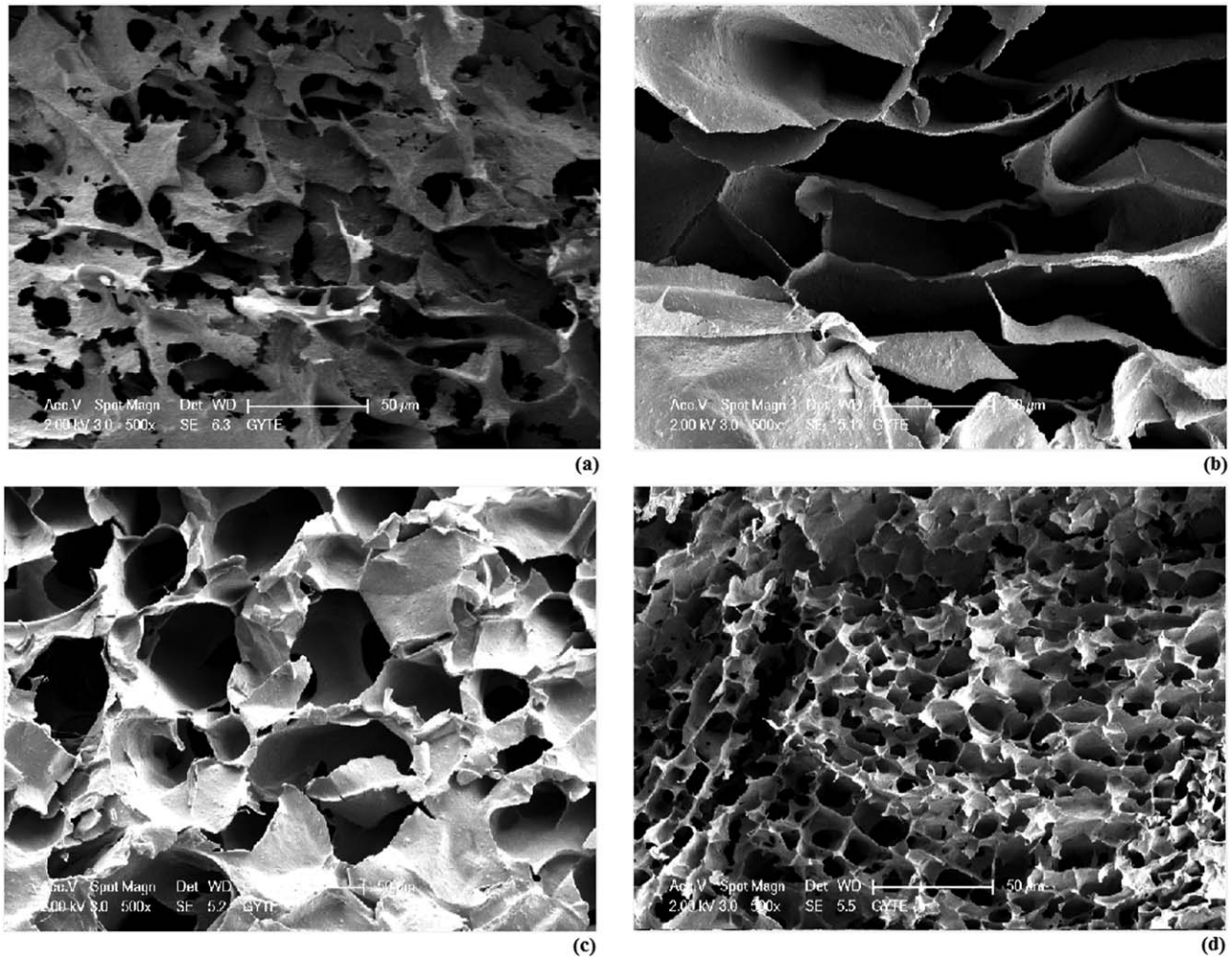

Figure 2. SEM micrographs of the nanocomposite hydrogels: (a) NaAlg10/PNIPA/Clay10, (b) NaAlg10/PNIPA/Clay15, (c) NaAlg10/PNIPA/Clay20, and (d) NaAlg10/PNIPA/Clay30. Scale bar is 50 μm. Magnification: 500×.

The deswelling behavior or water retention capacity of the hydrogels was studied by recording the weight of water in the hydrogels. Water retention capacity (WR, %) is given by:

$$\text{WR}\ (\%) = \frac{(W_t' - W_d)}{(W_s - W_d)} \times 100$$

where W_t' is the weight of the hydrogel at a given time during the course of deswelling after the swollen hydrogels at 5°C were quickly transferred into TRIS buffer at 37°C and pH = 6, and W_s is the weight of the equilibrium swollen hydrogel at 5°C.

The weights of the hydrogels were measured in every half an hour. All swelling and deswelling measurements were done in triplicates, and the average of three measurements is reported.

RESULTS AND DISCUSSION

Structure and Morphology of the Hydrogels

The hydrogels with different nanoclay contents were synthesized without any precipitation and phase separation (Figure 1). The prepared NaAlg*m*/PNIPA/Clay*n* hydrogels did not dissolve when they were put into an excess of water for a week at room temperature, but they swelled and kept their original shapes. This behavior is consistent with the results obtained by Haraguchi and Takehisa[26] and Ma *et al.*[31–33] This result showed that NIPA and nanoclay formed network structures without any organic cross-linker. As suggested by Haraguchi and Takehisa,[26] the initiator KPS strongly interacts with nanoclay sheets through ionic interactions and the KPS molecules were closely associated on the nanoclay surface in aqueous suspension. Radical formation was initiated followed by the propagation reaction, and thus the PNIPA chains were attached to the nanoclay sheets forming a cross-linked network structure. In order to prove that the nanoclay was cross-linked with the PNIPA and not the NaAlg, a mixture of the aqueous solution of nanoclay and NaAlg was prepared without PNIPA with the same procedure used in the preparation of NaAlg*m*/PNIPA/Clay*n* hydrogels. When the prepared material was immersed in an excess of water, NaAlg dissolved and a turbid solution was formed. This showed that NaAlg was not cross-linked by the nanoclay when there is no PNIPA in the hydrogel.

SEM micrographs of the freeze-dried NaAlg*m*/PNIPA/Clay*n* hydrogels are shown in Figure 2. The SEM micrographs of the nanocomposite hydrogels revealed a highly porous structure.

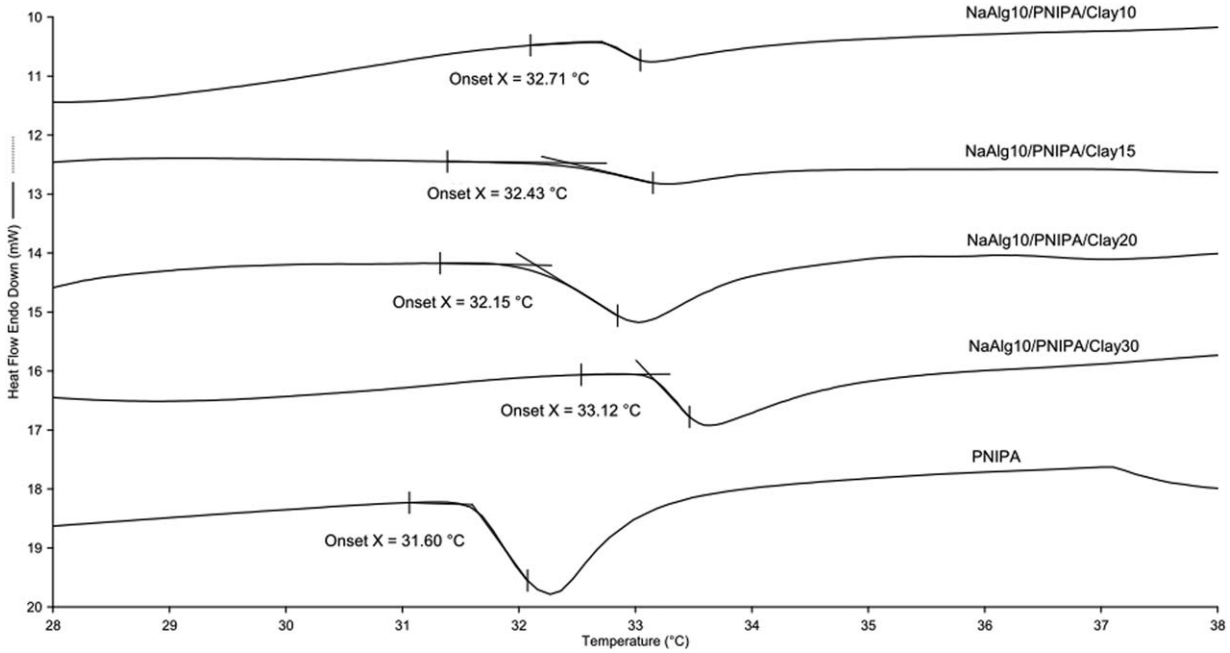

Figure 3. DSC thermograms of PNIPA and swollen NaAlg10/PNIPA/Clay*n* nanocomposite hydrogels. NaAlg20/PNIPA/Clay*n* hydrogels also showed similar behavior.

The pore size decreased and the amount of pores increased with increasing the nanoclay content in the hydrogels. Because the nanoclay sheets acted as a cross-linker, the increase in the amount of nanoclay in the hydrogels caused to form more cross-linking points in the polymer network, and thus resulted in hydrogels with lower pore size. Lee and Fu[34] also reported that the pore sizes of PNIPA/organic montmorillonite hydrogels cross-linked with *N,N′*-methylene-*bis*-acrylamide decreased and the amount of pores increased with an increase in the montmorillonite content in the hydrogels. Ma *et al.*[32] also reported similar results for carboxymethylcellulose/PNIPA/Clay nanocomposite hydrogels where pore size decreased with increasing the clay content in the hydrogels. The pore size and the amount of pores are important in swelling and deswelling characteristics of hydrogels. As the pore size decreases and the number of pores increases, the water diffuses out of the hydrogel more easily due to the presence of more water releasing channels when the temperature is above the LCST. The water penetration into the hydrogel matrix is restricted by more densely cross-linked network when the hydrogel has lower pore size and higher number of pores.

Thermal Analysis

LCST of the Hydrogels. The DSC thermograms of conventional PNIPA and NaAlg*m*/PNIPA/Clay*n* hydrogels are shown in Figure 3. The temperature at the onset point of the DSC endotherm is referred to as the LCST of the hydrogel.[35] The prepared nanocomposite hydrogels exhibited similar LCST values around 32.5°C, and the LCST of the PNIPA was 31.6°C which is very close to the LCST of the hydrogels. These results are consistent with the findings found by Zhang *et al.*,[21] Shi *et al.*[36] and Ma *et al.*[31] who reported that these hydrogels can be considered as semi-IPN systems. Because LCST of PNIPA and hydrogels are very close to each other indicating that there is no chemical bond between NaAlg and PNIPA network, which may change the balance between the hydrophobic and hydrophilic interactions in PNIPA. Our results showed PNIPA retained its own dehydration characteristics regardless of the amounts of NaAlg and nanoclay.

The NaAlg*m*/PNIPA/Clay*n* nanocomposite hydrogels changed their appearances from translucent to opaque by increasing the temperature from the equilibrium swollen state at 5 to 37°C, indicating that hydrogels were temperature sensitive (Figure 4). If the temperature was increased from a temperature below the LCST to a temperature above the LCST, PNIPA chains collapsed and shrunk due to the phase separation of PNIPA, resulting in a noticeable change in appearance of the hydrogel.[37,38]

Glass Transition of the Hydrogels. As shown in Figures 5 and 6, the T_g values of the dried NaAlg*m*/PNIPA/Clay*n* hydrogels ranged from 138.46 to 142.54°C. The T_g values of the dried

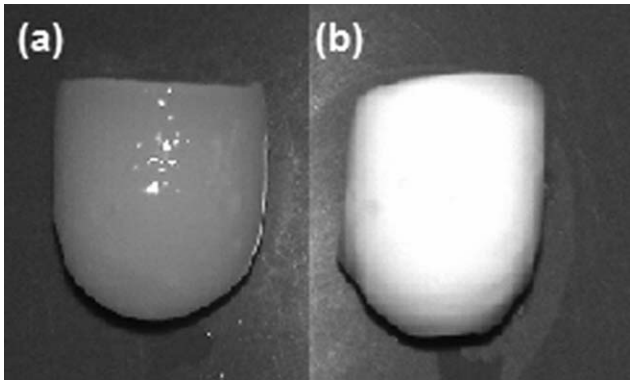

Figure 4. The appearance of the nanocomposite hydrogel (a) below and (b) above the LCST.

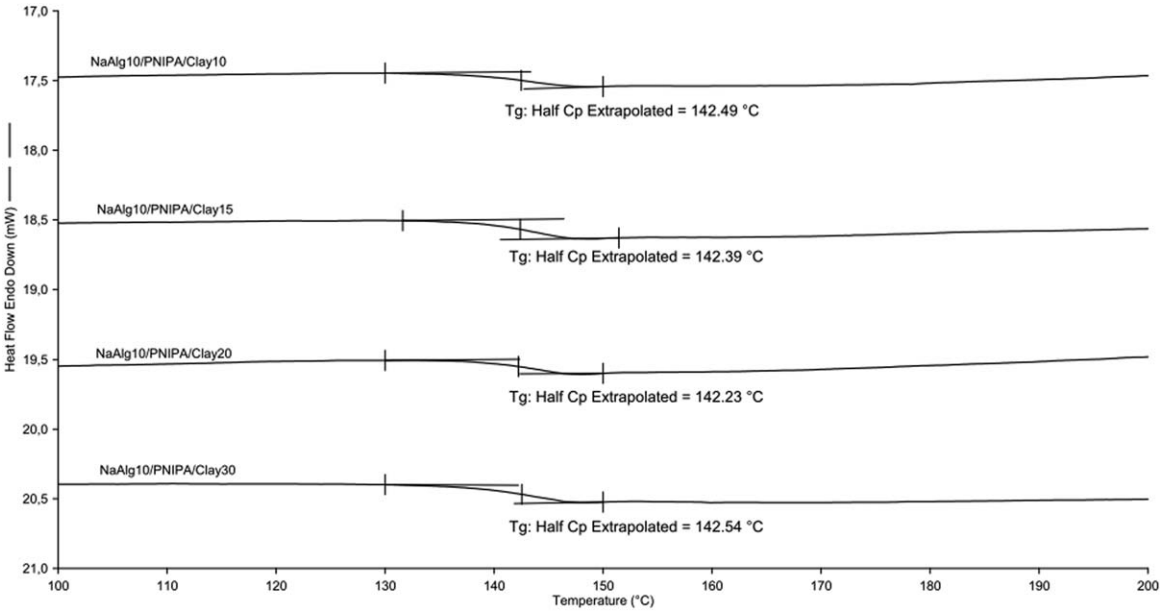

Figure 5. DSC thermograms of dried NaAlg10/PNIPA/Clay*n* nanocomposite hydrogels.

hydrogels did not change by increasing the amount of nanoclay in the hydrogels. The same observation was also made by Haraguchi and Takehisa[26] who showed that nanoclay content did not affect T_g in PNIPA/Clay hydrogels, but the T_g increased with increasing the amount of organic crosslinker in the hydrogels.

The relationship between the T_g values and the NaAlg content of the hydrogels was also investigated. The T_g of the dried hydrogels decreased from 142°C to 138°C with increasing the NaAlg content in the hydrogels from 10% to 20% (Figures 5 and 6). This can be interpreted that additional NaAlg might act as a plasticizer, hence lowering the T_g.

FT-NIR Analysis

The molecular structure of the nanocomposite hydrogels was investigated using FT-NIR spectroscopy which measures over- and combination-tones predominantly of the fundamental vibrations that involve hydrogen.[39] The combined FT-NIR spectra of NaAlg, nanoclay, PNIPA, and NaAlg*m*/PNIPA/Clay*n* nanocomposite hydrogels is shown in Figure 7. In the FT-NIR spectrum of NaAlg, a band between 4500 and 5000 cm^{-1} was attributed to combination of structural hydroxyl groups, and the peak at around 5175 cm^{-1} corresponds to first overtone of water molecules. The 4000 and 4400 cm^{-1} region includes the combination of asymmetric and symmetric –CH stretching vibrations in which the peak at 4290 cm^{-1} is because of

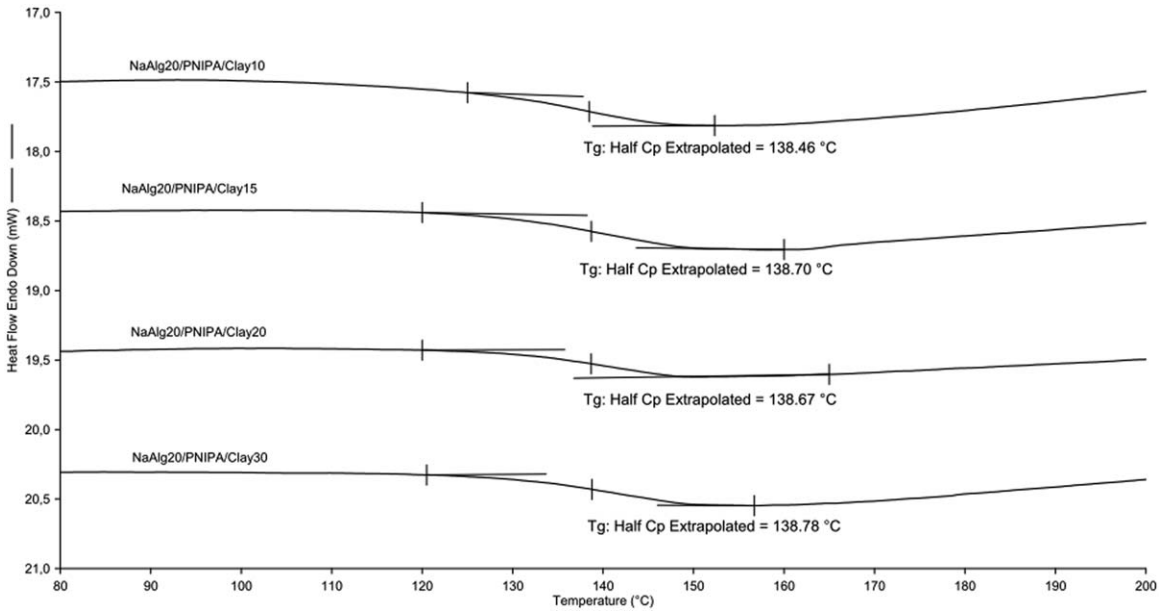

Figure 6. DSC thermograms of dried NaAlg20/PNIPA/Clay*n* nanocomposite hydrogels.

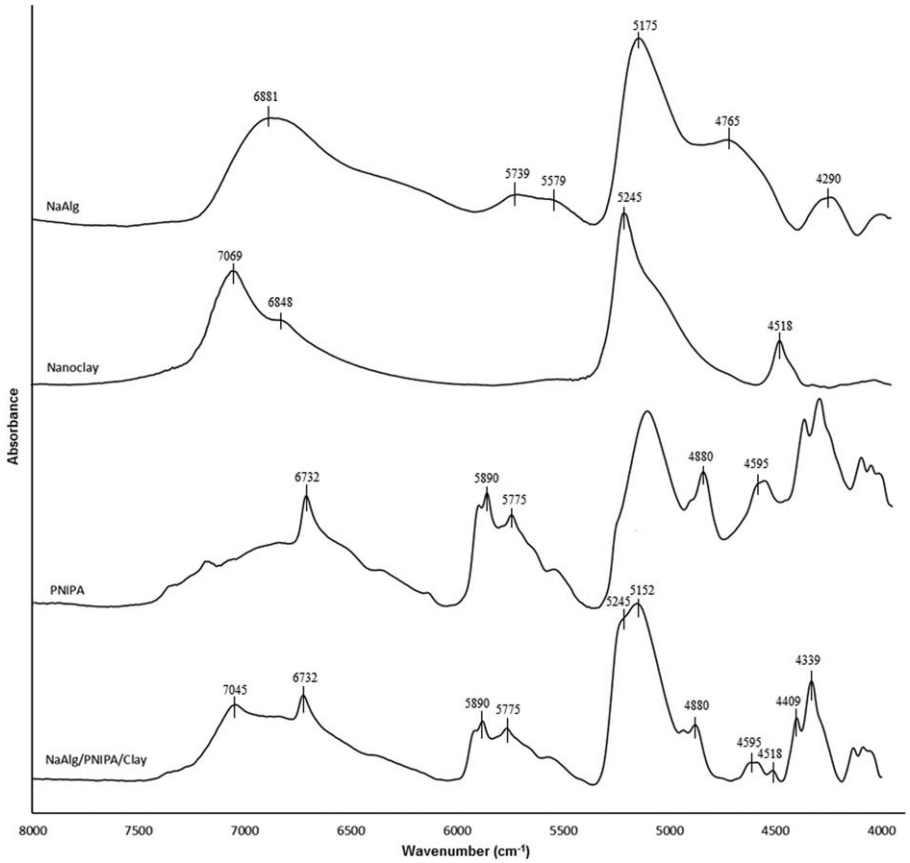

Figure 7. FT-NIR spectra of NaAlg, nanoclay, PNIPA, and NaAlg*m*/PNIPA/Clay*n* nanocomposite hydrogels.

combined stretching of –CH groups of NaAlg. A band between 5600 and 5900 cm^{-1} corresponds to first overtone of –CH vibrations, and a broad band between 6100 and 7300 cm^{-1} involves the second overtone of –CH combinations.

The FT-NIR spectrum of nanoclay was examined in two main regions corresponding to water signals. The first region between 4500 and 5500 cm^{-1} was attributed to the combination of water stretching modes and the water bending mode. The second region around 7000–7300 cm^{-1} corresponds to overtones of structural hydroxyl groups.[40,41] The shoulder near 6848 cm^{-1} is because of the first overtone of water molecules involved in strong hydrogen bonds.[42] The peak at 4518 cm^{-1} corresponds to combination of stretching vibrations for –SiOH groups.[43] In the spectrum of PNIPA, the absorption band at 4880 cm^{-1} corresponds to –NH/–CH stretch, and the peak at 4595 cm^{-1} and the large band from 5000 to 5300 cm^{-1} are attributed to –NH deformation overtones of PNIPA.

The FT-NIR spectrum of NaAlg*m*/PNIPA/Clay*n* hydrogel showed characteristic absorption bands present in nanoclay, NaAlg and PNIPA, indicating the presence of these substances in the hydrogel network. In the spectrum of NaAlg*m*/PNIPA/Clay*n* hydrogel, first overtone of –NH stretching peak appears at 6732 cm^{-1} which belongs to the PNIPA component in the hydrogel. The absorption band at 5775 cm^{-1} corresponds to first overtone of –CH stretching of the PNIPA.[44] In the spectra of NaAlg*m*/PNIPA/Clay*n* hydrogel, an intense complex band in the region of 5600–6100 cm^{-1} involves the contributions of overtones of asymmetric and symmetric stretching vibrations of CH_3 and CH_2 groups.[42] The peak at 5175 cm^{-1} in the NaAlg spectrum which is ascribed to first overtone of water molecules is shifted to 5152 cm^{-1} in the hydrogel spectrum of NaAlg*m*/PNIPA/Clay*n*, indicating increased hydrogen bonding interactions by the incorporation of nanoclay.[44] The peaks at 4518, 5245 and 7069 cm^{-1} are attributed to characteristic absorption peaks of nanoclay that appeared in the spectra of NaAlg*m*/PNIPA/Clay*n* nanocomposite hydrogel.

XRD Analysis

The XRD patterns of both nanoclay and freeze-dried nanocomposite hydrogels are shown in Figure 8. The basal spacing values for all samples were calculated by Bragg's Law ($n\lambda = 2d\sin\theta$). The nanoclay pattern displayed diffraction peaks at 2θ angle of 5.98° and 19.78° corresponded to a nanoclay interlayer spacing value of 1.48 and 0.45 nm, respectively. In the case of NaAlg*m*/PNIPA/Clay*n* nanocomposite hydrogels, the strength of the reflections tended to be weaker compared with nanoclay itself. In other words, the position of the diffraction peaks corresponding to nanoclay and nanocomposite hydrogels did not change, but the strength of the peaks became weaker when the nanoclay is incorporated into the hydrogel structure. If the polymer chains were intercalated between the nanoclay sheets, the XRD peaks for the nanocomposite hydrogels would be shifted to a lower angle. If the nanoclay sheets were completely

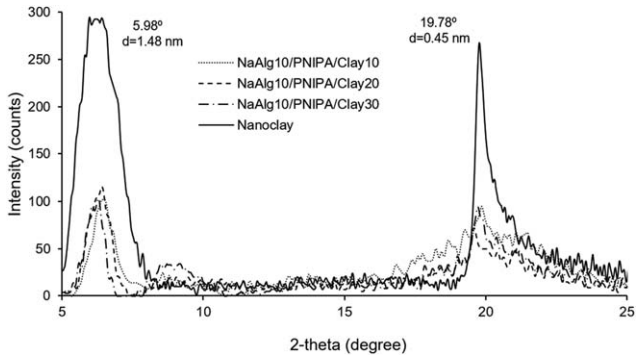

Figure 8. XRD profiles for nanoclay and NaAlg10/PNIPA/Clay*n* nanocomposite hydrogels. NaAlg20/PNIPA/Clay*n* hydrogels also showed similar behavior.

exfoliated in the hydrogel network, there would be no distinct diffraction peak. This implies that clay tactoids are broken up into more heterogeneous intercalated/exfoliated structures such as well aligned ordered and randomly disordered clay platelets.[45] Based on these XRD results, it could be suggested that some of the nanoclay sheets are exfoliated in the structure whereas some of exist as clay tactoids in the polymeric matrix.[46]

Effect of pH on Swelling

The effect of pH of the medium on the equilibrium swelling ratios of the hydrogels was studied in a pH range of 2 to 10 (Figure 9). The equilibrium swelling ratio of the nanocomposite hydrogels increased with increasing the pH from 2 to 6. At low pH values (below the $pK_a \cong 4.6$ of the carboxylic groups), the $-COO^-$ groups in NaAlg are protonated to form –COOH groups, and the hydrogen bonds between the –COOH groups in alginate and –CONH groups in PNIPA are formed.[21] Hydrogen bonds lead to polymer-polymer interactions predominating over the polymer-water interactions which result in a decrease of swelling ratios.[21] When the pH is above the pK_a value of the carboxylic groups, the carboxylic groups become ionized and the electrostatic repulsions among the molecular chains is predominated which leads to the network to expand. This increases the diffusion of water molecules into the hydrogel until the maximum swelling ratio is attained at pH of 6[2131,33]. At pH = 6, all the –COOH groups were converted to $-COO^-$ groups, and this resulted in high anion-anion repulsions and high swelling ratio. Above pH of 6, a screening effect of counter ions, such as Na^+, shielded the $-COO^-$ groups and prevented anion-anion repulsions, resulting in limited water diffusion into the hydrogel. As a result, a significant decrease in equilibrium swelling occurred. Ma *et al.*[47] reported similar results for carboxymethylcellulose/PNIPA/clay nanocomposite hydrogels where maximum swelling ratio was attained at pH = 5.9 because both alginate and carboxymethylcellulose have carboxylic groups. Pourjavadi *et al.*[48] also found that alginate-*g*-poly(sodium acrylate)/kaolin nanocomposite hydrogels reached maximum swelling ratio at pH = 8.

Effect of Nanoclay on Swelling

Equilibrium swelling ratios of the hydrogels with different nanoclay contents at pH of 6 where maximum swelling is attained are shown in Figure 10. When the nanoclay content was 10% in the hydrogel, there was no difference in the equilibrium swelling ratios of the hydrogels containing 10% and 20% NaAlg. When the nanoclay content was increased to 20%, there was an incremental decrease in the equilibrium swelling ratios of the hydrogels compared to the hydrogels with 10% nanoclay. Further increase in the nanoclay caused a decrease in the swelling ratios of the hydrogels which is because of the high cross-linking as confirmed by SEM analysis and studies conducted in excess of water with the polymer network without any organic cross-linker. When the amount of nanoclay in the hydrogel was increased to 30%, the polymer chains in the hydrogel were restricted by a large number of chemical cross-links because of the nanoclay, resulting in a polymer network with less swelling ratio.[27,33,49] In other words, increasing the nanoclay content caused to decrease the cross-linking distance between polymer chains, resulting in the formation of denser polymeric network with less water swelling as confirmed by SEM images. Similar results were also reported by Li *et al.*[50] who found that the equilibrium swelling ratio of poly(acrylamide)/PNIPA/Laponite hydrogels decreased as the nanoclay content in the hydrogel was increased. Mahdavinia *et al.*[23] observed a similar swelling behavior for poly(acrylamide)/carrageenan/Montmorillonite hydrogels where they reported that high clay concentration increased the extent of cross-linking of the polymer network, resulting in less swelling. Ma *et al.*[33] also found that the equilibrium swelling ratios of carboxymethylcellulose/PNIPA/Laponite hydrogels in a

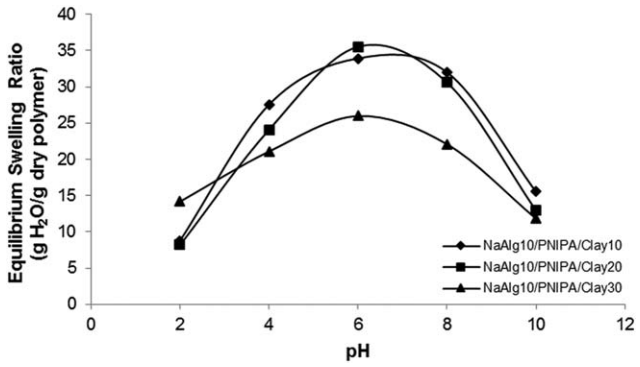

Figure 9. pH dependent swelling behavior of the NaAlg*m*/PNIPA/Clay*n* nanocomposite hydrogels at 5°C.

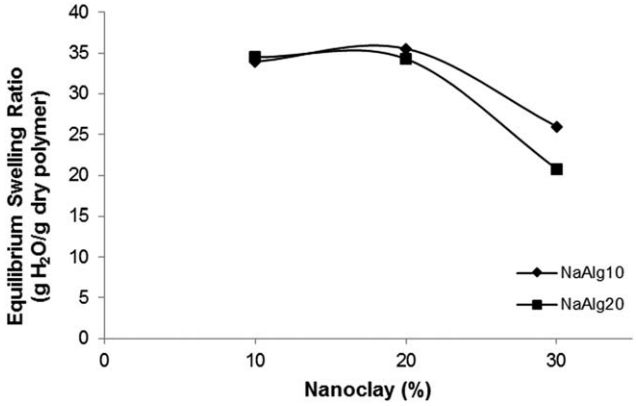

Figure 10. The effect of nanoclay content on the swelling behavior of NaAlg*m*/PNIPA/Clay*n* nanocomposite hydrogels at 5°C and pH = 6.

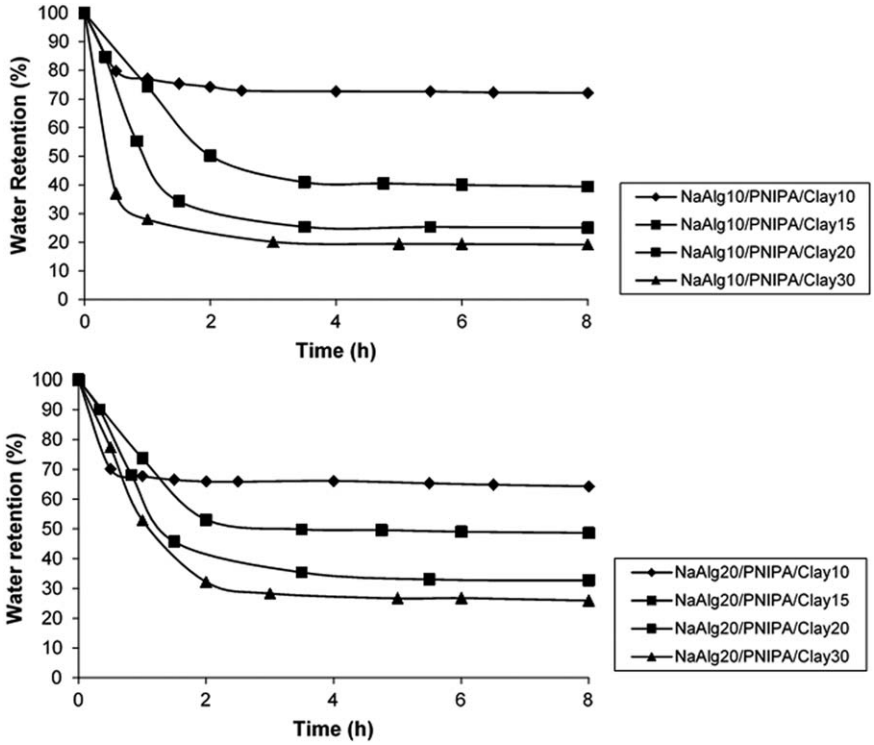

Figure 11. Deswelling characteristics of the NaAlg*m*/PNIPA/Clay*n* hydrogels at 37°C in buffer solution with pH = 6.

medium at pH = 1.2 and 7.4 decreased as the clay content increased from 20 to 60%.

Deswelling Behavior of Hydrogels in Response to Temperature Change

NaAlg*m*/PNIPA/Clay*n* hydrogels were taken from the swelling medium at 5°C and put in a medium at 37°C, and their deswelling behaviors were investigated (Figure 11). The deswelling rates increased with increasing the nanoclay content. The hydrogels with 10% nanoclay showed minimum deswelling while the hydrogels with 30% nanoclay showed maximum deswelling. These results are in agreement with the findings reported by Lee and Fu[34] who also observed that the deswelling rate of PNIPA/Clay hydrogels increased as the clay content increased from 1 to 20%. The increase in deswelling rate with an increase in nanoclay content could be attributed to the formation of more porous structure within the hydrogels as confirmed by SEM studies. In other words, more nanoclay incorporation into the hydrogels led to the formation of more porous structure in which high number of pores provides more water releasing channels so the water molecules can be squeezed out of the hydrogel more easily at temperatures above the LCST.[32,34] These results suggest that it is possible to design a hydrogel with a desired deswelling behavior by controlling the nanoclay content in the hydrogel.

CONCLUSION

Semi-IPN NaAlg*m*/PNIPA/Clay*n* nanocomposite hydrogels were synthesized by free radical solution polymerization. The bentonite nanoclay acted as a cross-linker instead of organic cross-linkers. The nanocomposite hydrogels were characterized by SEM, DSC, FT-NIR and XRD methods. SEM pictures of the nanocomposite hydrogels revealed a highly porous structure. The pore sizes decreased and the amount of pores increased with increasing the nanoclay content in the hydrogels. DSC thermograms of the nanocomposite hydrogels exhibited similar LCST values around 32.5°C as that of the conventional PNIPA hydrogel which has a LCST of 31.6°C very close to the LCST of the nanocomposite hydrogels. FT-NIR spectrum of NaAlg*m*/PNIPA/Clay*n* hydrogels showed the characteristic absorptions of nanoclay, NaAlg and PNIPA, indicating the presence of these substances in the hydrogel network. The XRD profiles of nanocomposite hydrogels revealed that some of the nanoclay sheets are exfoliated in the structure whereas some of exist as clay tactoids in the polymeric matrix. The degree of swelling was affected by the pH of the swelling medium and the nanoclay content in the hydrogel. The equilibrium swelling ratios of the nanocomposite hydrogels increased with increasing the pH from 2 to 6 where the maximum swelling was obtained. There was no change in the equilibrium swelling ratios of the hydrogels when the nanoclay content is 10% while an increase in the nanoclay content from 20 to 30% caused a decrease in the equilibrium swelling ratio. The deswelling rate increased as the nanoclay content increased in the hydrogel. The increase in deswelling rate with an increase in nanoclay content could be attributed to the formation of more porous structure within the hydrogels. The results indicated that the synthesized nanocomposite hydrogels have good water holding capacity which can be adjusted by controlling the amount of nanoclay in the hydrogel.

Compared with the conventional organically cross-linked hydrogels, this study more deeply focuses on the effects of nanoclay on the characteristics of NaAlg/PNIPA/Clay hydrogels. The nanocomposite hydrogels prepared in this study have high swelling and deswelling ability enabling them to be used as matrixes for the entrapment and delivery of proteins, drugs, and active agents. These hydrogels have high porosity that allows more molecules to diffuse in the hydrogels without the use of any pore forming agent. They can be used as smart delivery devices that can be incorporated into intelligent packaging systems. They can also be used to control the release of food preservatives as a response to temperature and pH changes during the storage of foods, thereby minimizing spoilage and prolonging the shelf-life while maintaining the nutritional quality of foods. These hydrogels can potentially be used in food, agricultural, and biochemical products and pharmaceuticals.

ACKNOWLEDGMENTS

This work was financially supported by Gebze Technical University through Scientific Research Project (BAP) 2011 A-23.

REFERENCES

1. Buchholz, F. L. In Modern Superabsorbent Polymer Technology; Buchholz, F. L., Graham, A. T., Eds.; Wiley: New York, **1998**, 252.
2. Feil, H.; Bae, Y. H.; Feijen, J.; Kim, S. W. *J. Membr. Sci.* **1991**, *64*, 283.
3. Leach, J. B.; Schmidt, C. E. *Biomaterials* **2005**, *26*, 125.
4. Balakrishnan, B.; Mohanty, M.; Umashankar, P. R.; Jayakrishnan, A. *Biomaterials* **2005**, *26*, 6335.
5. Chen, S. C.; Wu, Y. C.; Mi, F. L.; Lin, Y. H.; Yu, L. C.; Sung, H. W. *J. Control. Release* **2004**, *96*, 285.
6. Guilherme, M. R.; Reis, A. V.; Paulino, A. T.; Moia, T. A.; Mattoso, L. H. C.; Tambourgi, E. B. *J. Appl. Polym. Sci.* **2010**, *117*, 3146.
7. Roy, N.; Saha, N.; Kitano, T.; Saha, P. *Carbohydr. Polym.* **2012**, *89*, 346.
8. Deng, K. L.; Wang, S. L.; Li, Q.; Cheng, H.; Zhang, P. F.; Gao, T.; Huang, C. Y.; Li, C. X. *Appl. Mech. Mater.* **2011**, *117*, 1429.
9. Xu, X.; Song, J.; Wang, K.; Gu, Y. C.; Luo, F.; Tang, X. H.; Xie, P.; Qian, Z. Y. *Macromol. Res.* **2013**, *21*, 870.
10. Schmaljohann, D. *Adv. Drug Deliv. Rev.* **2006**, *58*, 1655.
11. Malonne, H.; Eeckman, F.; Fontaine, D.; Otto, A.; De Vos, L.; Moes, A.; Fontaine, J.; Amighi, K. *Eur. J. Pharm. Biopharm.* **2005**, *61*, 188.
12. Schild, H. G. *Prog. Polym. Sci.* **1992**, *17*, 163.
13. Kim, J. H.; Lee, S. B.; Kim, S. J.; Lee, Y. M. *Polymer* **2002**, *43*, 7549.
14. Yang, H.; Wang, W.; Wang, A. *J. Dispersion Sci. Technol.* **2012**, *33*, 1154.
15. Culin, J.; Smit, I.; Andreis, M.; Veksli, Z.; Anzlovar, A.; Zigon, M. *Polymer* **2005**, *46*, 89.
16. Ma, J. H.; Fan, B.; Liang, B. R.; Xu, J. *J. Colloid Interface Sci.* **2010**, *341*, 88.
17. Zhang, J.; Peppas, N. A. *Macromolecules* **2000**, *33*, 102.
18. Song, L. Y.; Zhu, M. F.; Chen, Y. M.; Haraguchi, K. *Macromol. Chem. Phys.* **2008**, *209*, 1564.
19. Lee, W. F.; Chen, Y. J. *J. Appl. Polym. Sci.* **2001**, *82*, 2487.
20. Guo, B. L.; Gao, Q. Y. *Carbohydr. Res.* **2007**, *342*, 2416.
21. Zhang, G. Q.; Zha, L. S.; Zhou, M. H.; Ma, J. H.; Liang, B. R. *Colloid Polym. Sci.* **2005**, *283*, 431.
22. Jordan, J.; Jacob, K. I.; Tannenbaum, R.; Sharaf, M. A.; Jasiuk, I. *Mat. Sci. Eng. A Struct.* **2005**, *393*, 1.
23. Mahdavinia, G. R.; Marandi, G. B.; Pourjavadi, A.; Kiani, G. *J. Appl. Polym. Sci.* **2010**, *118*, 2989.
24. Haraguchi, K. *Curr. Opin. Solid State Mater. Sci.* **2007**, *11*, 47.
25. Zhang, Q. S.; Li, X. W.; Zhao, Y. P.; Chen, L. *Appl. Clay Sci.* **2009**, *46*, 346.
26. Haraguchi, K.; Takehisa, T. *Adv. Mater.* **2002**, *14*, 1120.
27. Haraguchi, K.; Takehisa, T.; Fan, S. *Macromolecules* **2002**, *35*, 10162.
28. Haraguchi, K.; Li, H. J.; Matsuda, K.; Takehisa, T.; Elliott, E. *Macromolecules* **2005**, *38*, 3482.
29. Haraguchi, K.; Li, H. J. *Macromolecules* **2006**, *39*, 1898.
30. Zhang, J.; Wang, A. *React. Funct. Polym* **2007**, *67*, 737.
31. Ma, J. H.; Xu, Y. J.; Zhang, Q. S.; Zha, L. S.; Liang, B. R. *Colloid Polym. Sci.* **2007**, *285*, 479.
32. Ma, J.; Zhang, L.; Li, Z.; Liang, B. *Polym. Bull.* **2008**, *61*, 593.
33. Ma, J. H.; Zhang, L.; Fan, B.; Xu, Y. J.; Liang, B. R. *J. Polym. Sci. B: Polym. Phys.* **2008**, *46*, 1546.
34. Lee, W. F.; Fu, Y. T. *J. Appl. Polym. Sci.* **2003**, *89*, 3652.
35. Otake, K.; Inomata, H.; Konno, M.; Saito, S. *Macromolecules* **1990**, *23*, 283.
36. Shi, J.; Alves, N. M.; Mano, J. F. *Macromol. Biosci.* **2006**, *6*, 358.
37. Feil, H.; Bae, Y. H.; Feijen, J.; Kim, S. W. *Macromolecules* **1993**, *26*, 2496.
38. Zhang, J. T.; Huang, S. W.; Zhuo, R. X. *Macromol. Biosci.* **2004**, *4*, 575.
39. Salomonsen, T.; Jensen, H. M.; Stenbæk, D.; Engelsen, S. B. *Carbohydr. Polym.* **2008**, *72*, 730.
40. Tomic, Z. P.; Asanin, D.; Antic-Mladenovic, S.; Poharc-Logar, V.; Makreski, P. *Vib. Spectrosc.* **2012**, *58*, 95.
41. Rinnert, E.; Carteret, C.; Humbert, B.; Fragneto-Cusani, G.; Ramsay, J. D. F.; Delville, A.; Robert, J. L.; Bihannic, I.; Pelletier, M.; Michot, L. J. *J. Phys. Chem. B* **2005**, *109*, 23745.
42. Madejová, J.; Pálková, H.; Jankovič, Ľ. *Mater. Chem. Phys.* **2012**, *134*, 768.
43. Holmes, P. A. In Eurogel '91: Progress in Research and Development of Processes and Products from Sols and Gels; Vilminot, S., Nass, R., Schmidt, H., Eds.; Elsevier Science Publishers: Amsterdam, **1995**, 181.
44. Nistor, M. T.; Chiriac, A. P.; Nita, L. E.; Vasile, C. *Int. J. Pharm.* **2013**, *452*, 92.

45. Dong, Y.; Bhattacharyya, D. *Composites A* **2008**, *39*, 1177.
46. Wang, X.; Yang, L.; Zhang, J.; Wang, C.; Li, Q. *Chem. Eng. J.* **2014**, *251*, 404.
47. Ma, J.; Xu, Y.; Fan, B.; Liang, B. *Eur. Polym. J.* **2007**, *43*, 2221.
48. Pourjavadi, A.; Ghasemzadeh, H.; Soleyman, R. *J. Appl. Polym. Sci.* **2007**, *105*, 2631.
49. Xiang, Y.; Peng, Z.; Chen, D. *Eur. Polym. J.* **2006**, *42*, 2125.
50. Li, B.; Jiang, Y.; Liu, Y.; Wu, Y.; Yu, H.; Zhu, M. *J. Polym. Sci. Part B: Polym. Phys.* **2009**, *47*, 96.